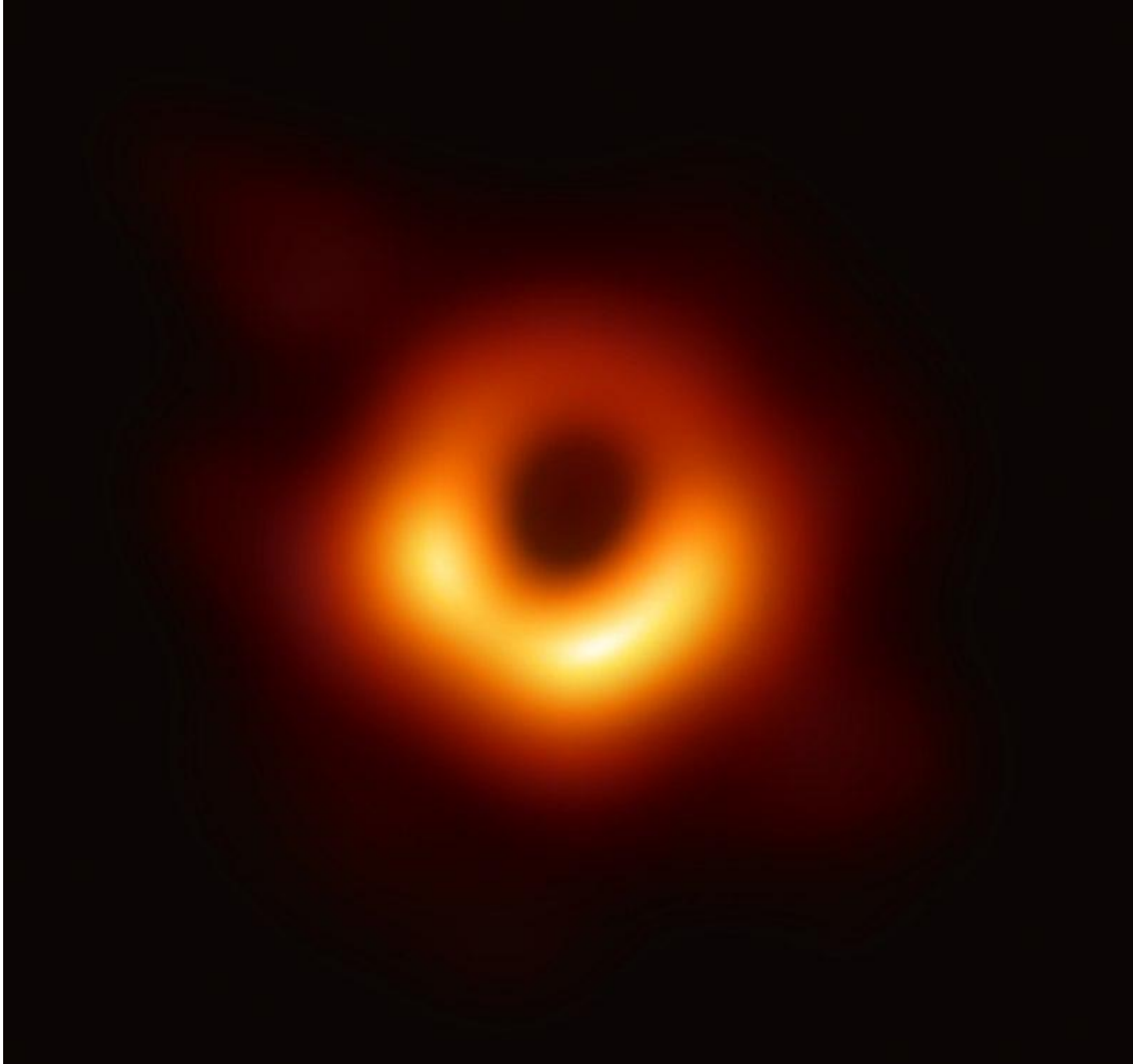


INVESTIGATING PRIMORDIAL BLACK HOLES

**GIULIO SCELFO
SISSA**

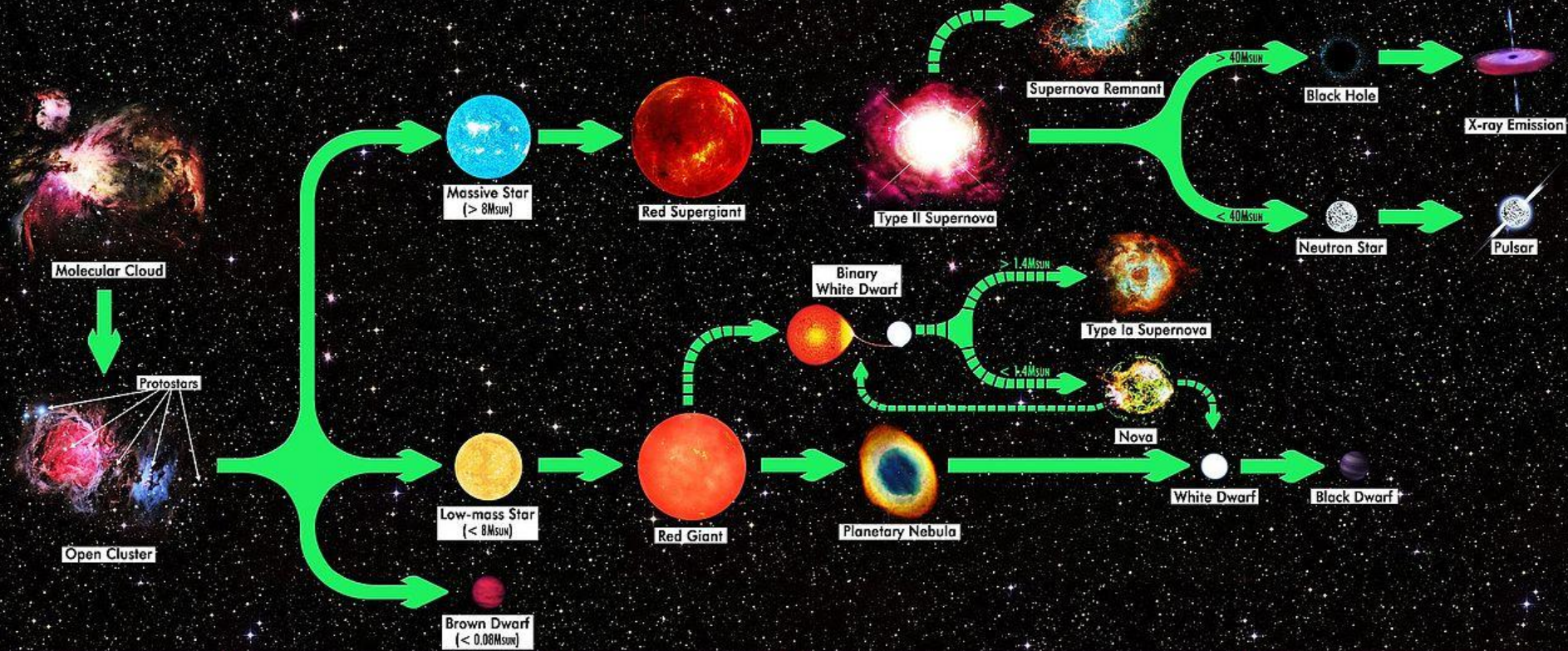
SUPERVISORS: M. VIEL, A. LAPI

ASTRO@TS 2019



M87 supermassive Black Hole (Event Horizon Telescope)

STELLAR LIFE CYCLE



Birth

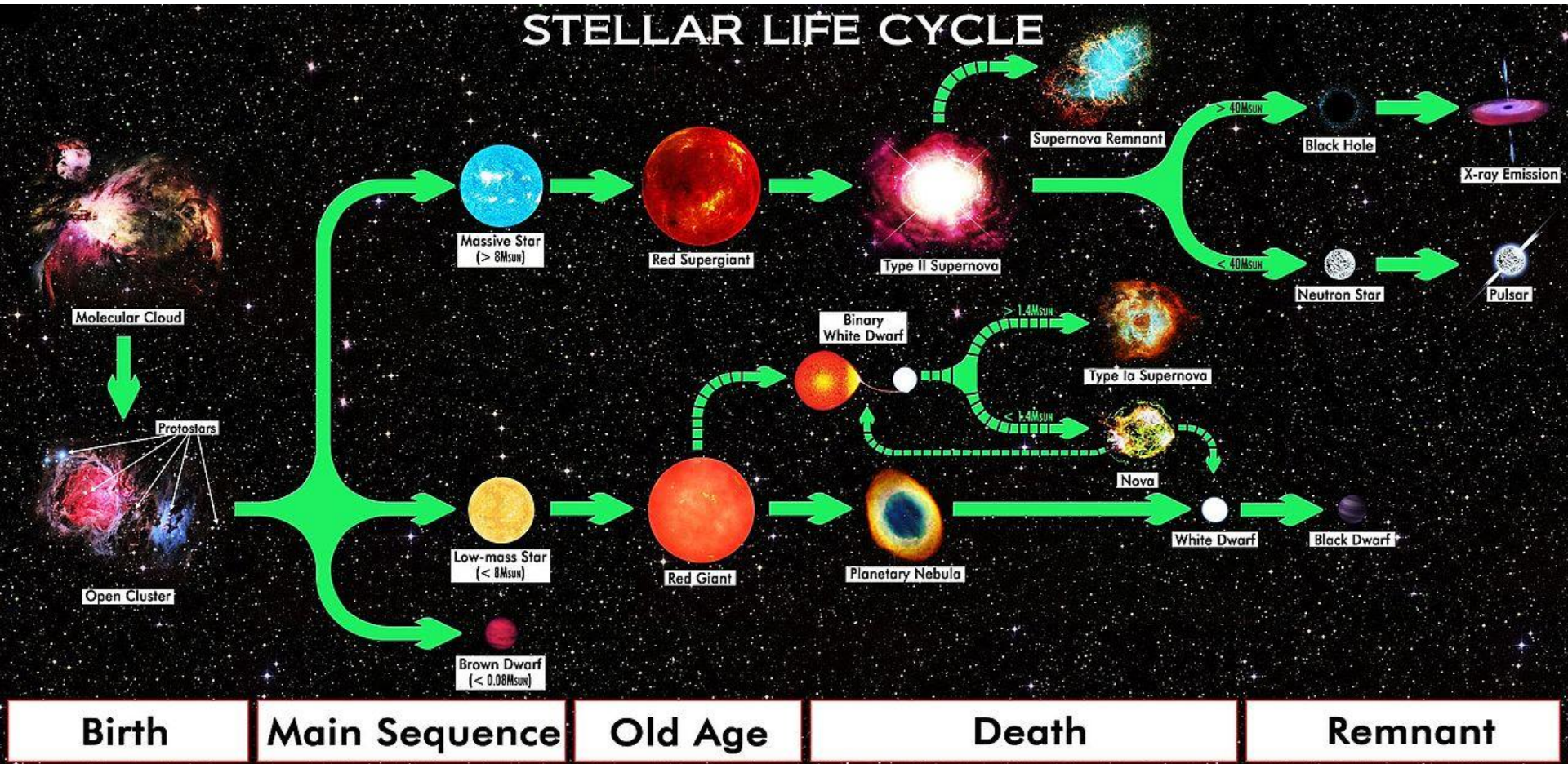
Main Sequence

Old Age

Death

Remnant

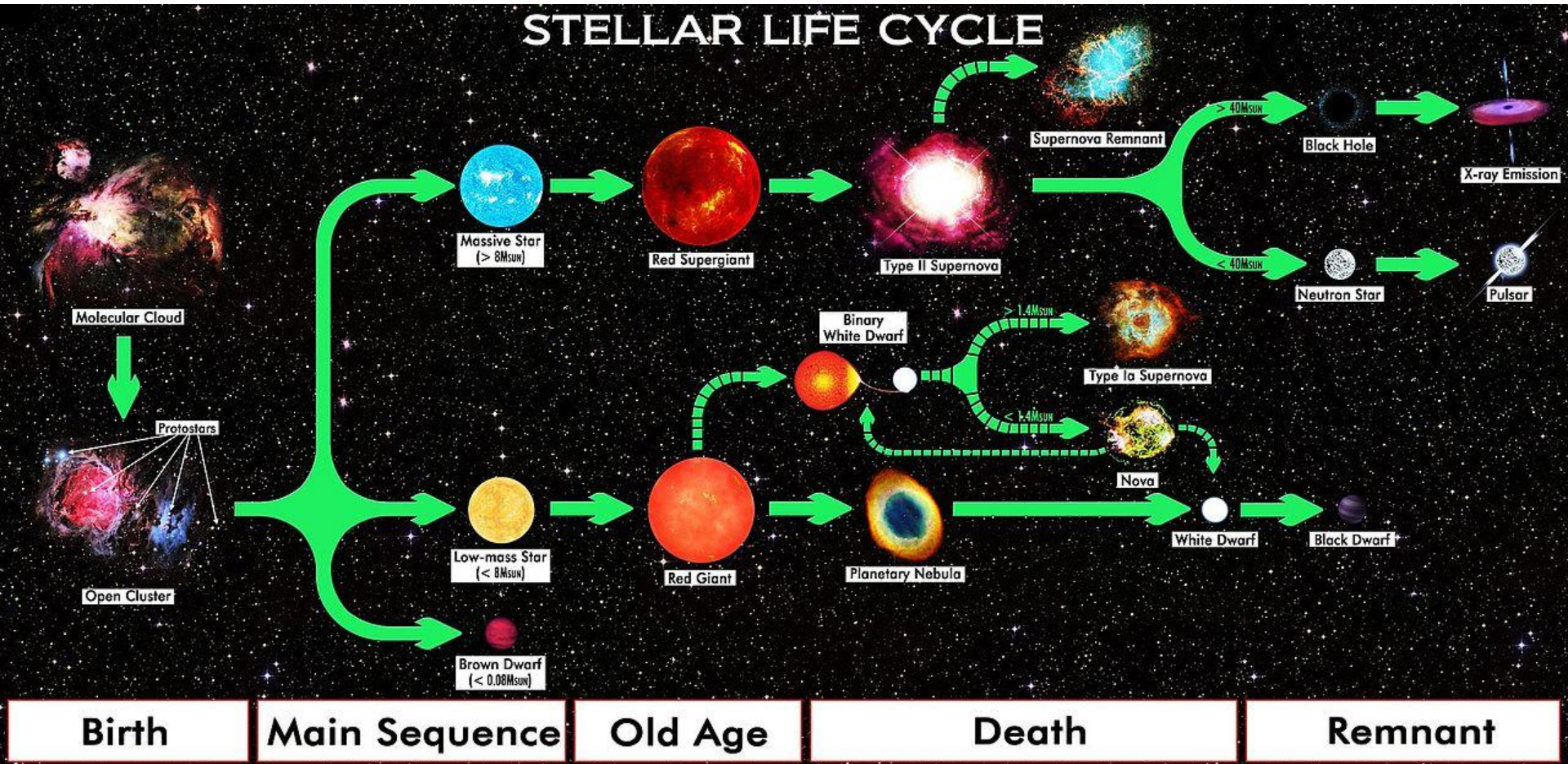
STELLAR LIFE CYCLE



Could there be another way to form BHs?

High density environment...

STELLAR LIFE CYCLE



Could there be another way to form BHs?

High density environment...

EARLY UNIVERSE!

THE HYPOTHESIS OF CORES RETARDED DURING EXPANSION AND THE HOT COSMOLOGICAL MODEL

Ya. B. Zel'dovich and I. D. Novikov

Translated from *Astronomicheskii Zhurnal*, Vol. 43, No. 4,
pp. 758-760, July-August, 1966
Original article submitted March 14, 1966

**Highly overdense
regions** in the
primordial Universe
can directly undergo
gravitational collapse
to **form BHs**.

GRAVITATIONALLY COLLAPSED OBJECTS OF VERY LOW MASS

Stephen Hawking

(Communicated by M. J. Rees)

(Received 1970 November 9)

PBHs **dimentions** of
the **order of the
particle horizon** at
formation time.

BLACK HOLES IN THE EARLY UNIVERSE

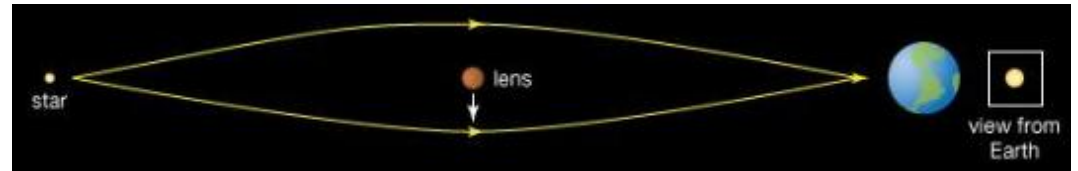
B. J. Carr and S. W. Hawking

(Received 1974 February 25)

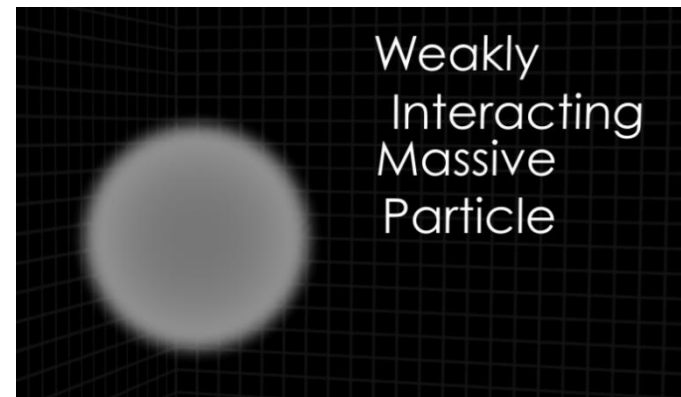
PBHs would not grow
significantly after
fomation.

COULD PBHs BE THE DARK MATTER WE ARE LOOKING FOR?

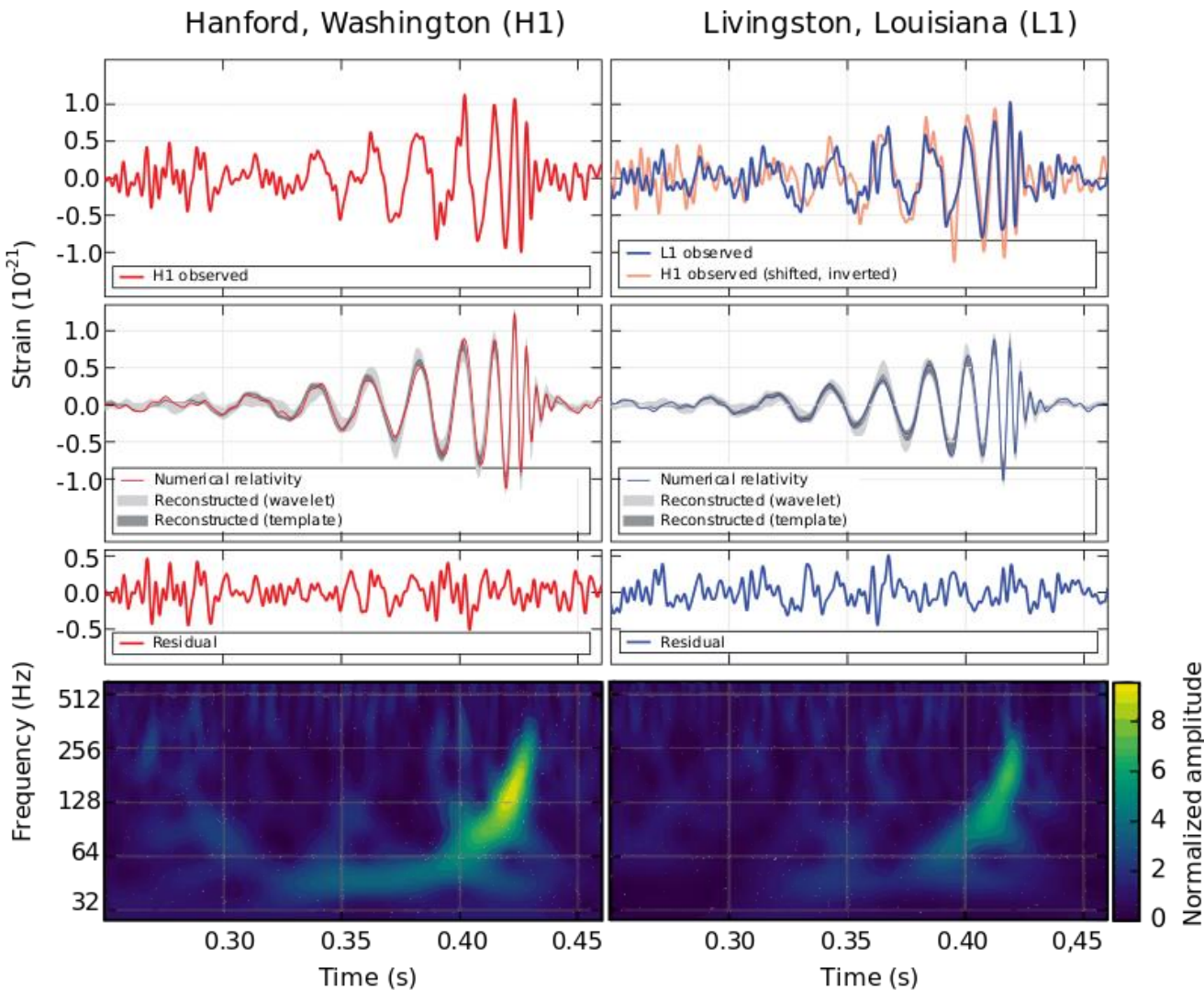
- MACHOS constraints



- Rise of WIMP model



“**PBHs as DM**” hypothesis lost interest, *until...*



BHs merger
detected
through GWs!

$$36^{+5}_{-4} M_{\odot}$$

$$29^{+4}_{-4} M_{\odot}$$

GW150914 (1602.03837)

Less constrained mass window to have PBHs composing significant fraction of DM:

$$20 M_{\odot} \lesssim M_{\text{PBH}} \lesssim 100 M_{\odot}$$

Did LIGO detect dark matter?

Simeon Bird,* Ilias Cholis, Julian B. Muñoz, Yacine Ali-Haïmoud, Marc Kamionkowski, Ely D. Kovetz, Alvise Raccanelli, and Adam G. Riess¹

¹*Department of Physics and Astronomy, Johns Hopkins University,
3400 N. Charles St., Baltimore, MD 21218, USA*



Predicted **merger rate** in the “PBHs as DM” scenario:

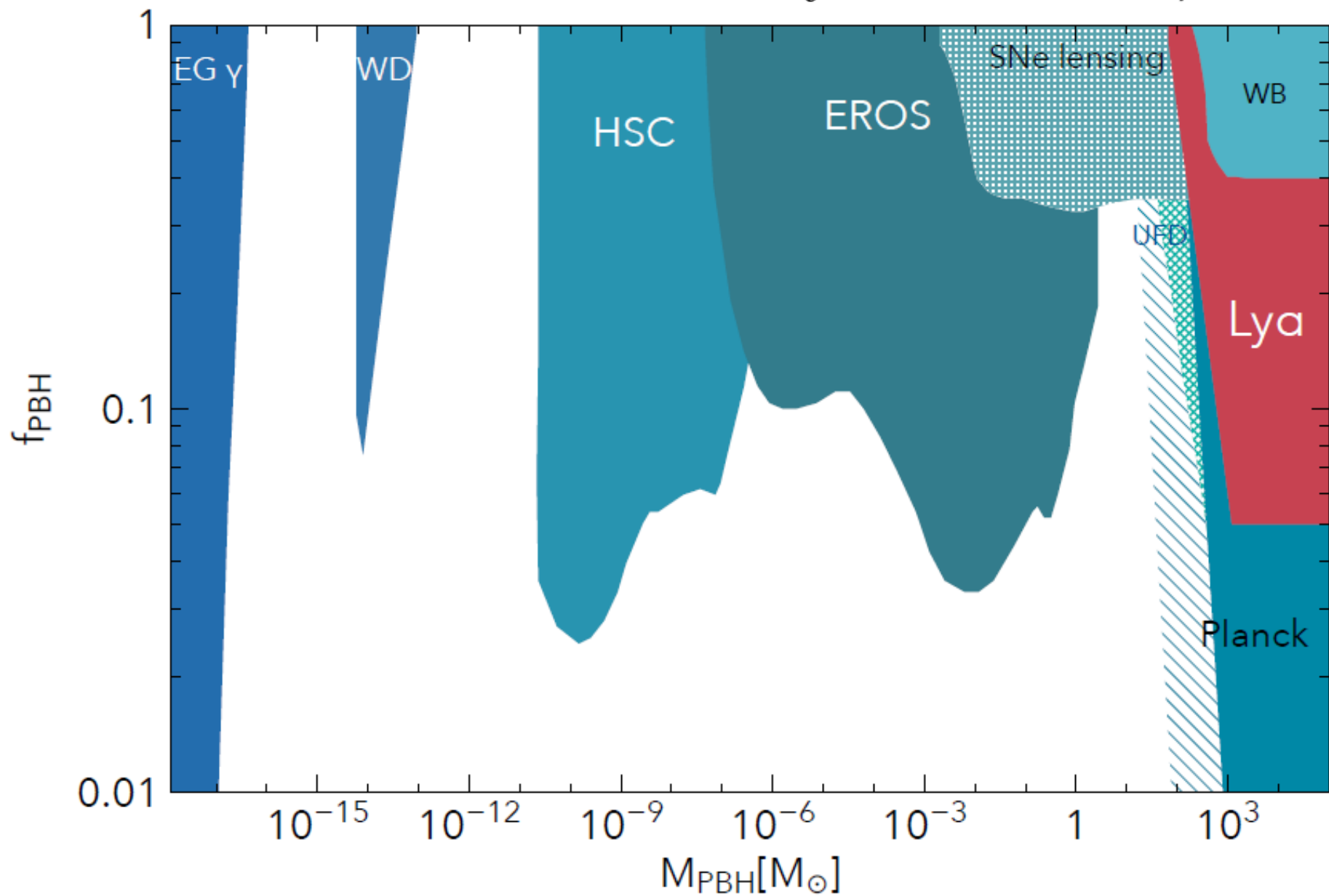
IN AGREEMENT WITH LIGO VALUE!



**REVIVED INTEREST
TOWARDS PBHs!**

What's the situation today?

$$f_{\text{PBH}} \equiv \Omega_{\text{PBH}} / \Omega_{\text{DM}}$$



Lyman- α forest constraints on Primordial Black Holes as Dark Matter

Riccardo Murgia,^{1,2,3} Giulio Scelfo,^{1,2,3} Matteo Viel,^{1,2,3,4} and Alwise Raccanelli⁵

¹*SISSA, Via Bonomea 265, 34136 Trieste, Italy*

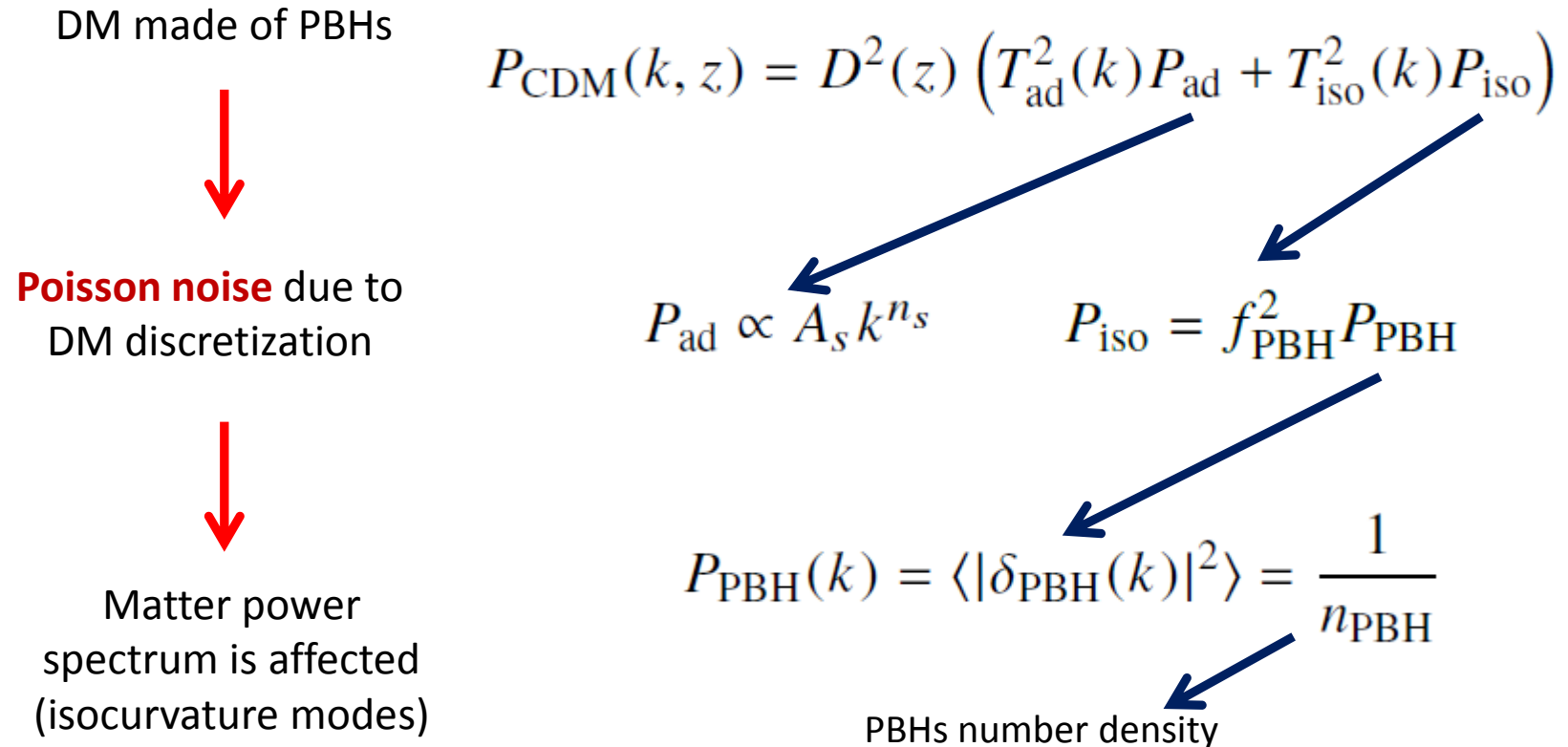
²*INFN, Sezione di Trieste, Via Bonomea 265, 34136 Trieste, Italy*

³*IFPU, Institute for Fundamental Physics of the Universe, via Beirut 2, 34151, Trieste, Italy*

⁴*INAF/OATS, Osservatorio Astronomico di Trieste, via Tiepolo 11, I-34143 Trieste, Italy*

⁵*Theoretical Physics Department, CERN, 1 Esplanade des Particules, CH-1211 Geneva 23, Switzerland*

Updated results from *Afshordi et al. (2003)*, improving constraints by 2 orders of magnitude.



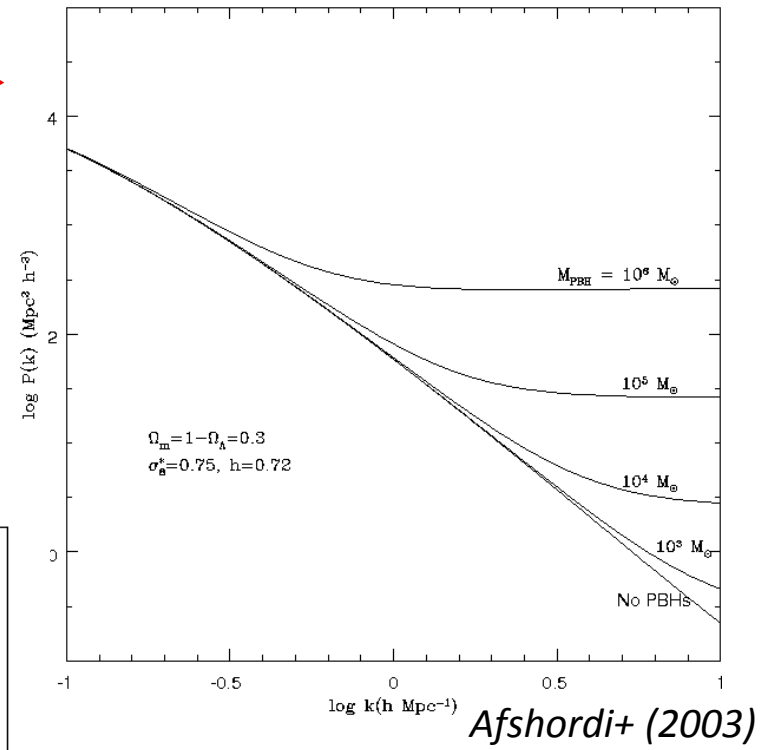
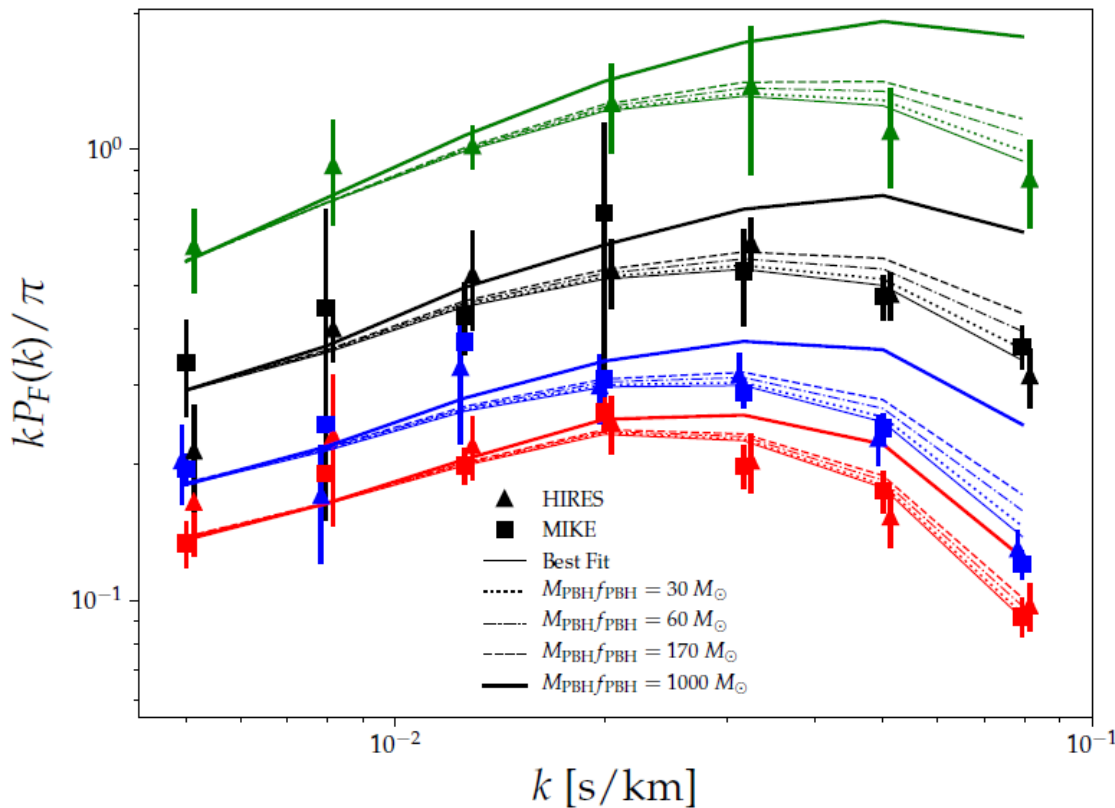
Effect of PBHs on **linear matter power spectrum**



Lyman-a forest Flux Power Spectrum is affected



Murgia, GS, Viel, Raccanelli (2019)



Lyman-a forest:
 series of absorption lines
 in the spectra of
 distant galaxies
 and quasars arising from
 Lyman-a electron
 transition of
neutral hydrogen.

Hydrodynamic simulations.

MCMC

High-resolution, high-redshift
Lyman- α forest data
(MIKE/HIRES).

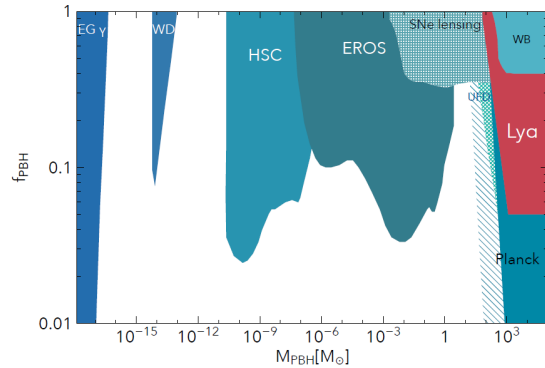
UPPER LIMIT ON PBHs MASS.

ALLOWED PARAMETER SPACE:

$$f_{\text{PBH}} M_{\text{PBH}} \lesssim 170 M_{\odot} (2\sigma)$$

Adding data motivated Gaussian prior on reionization z :

$$f_{\text{PBH}} M_{\text{PBH}} \lesssim 60 M_{\odot} (2\sigma)$$



CONCLUSIONS

- PBHs studies can provide insights into several aspects in Physics, **whether they constitute all the DM or not.**
- PBHs **constraints** are still **far from conclusive.**
- **Lyman-alpha** constraints can rule out upper part of masses in the LIGO range.

THANK YOU FOR
YOUR ATTENTION!

BACKUP SLIDES

$$P_{\text{CDM}}(k, z) = D^2(z) \left(T_{\text{ad}}^2(k) P_{\text{ad}} + T_{\text{iso}}^2(k) P_{\text{iso}} \right)$$

$$P_{\text{ad}} \propto A_s k^{n_s} \quad P_{\text{iso}} = f_{\text{PBH}}^2 P_{\text{PBH}} = \frac{2\pi^2}{k^3} A_{\text{iso}} \left(\frac{k}{k_*} \right)^{n_{\text{iso}}-1}$$

$$P_{\text{PBH}}(k) = \langle |\delta_{\text{PBH}}(k)|^2 \rangle = \frac{1}{n_{\text{PBH}}}$$

$$f_{\text{iso}} = \sqrt{\frac{A_{\text{iso}}}{A_s}} = \sqrt{\frac{k_*^3 f_{\text{PBH}}^2}{2\pi^2 n_{\text{PBH}}} \frac{1}{A_s}} = \sqrt{\frac{k_*^3 M_{\text{PBH}} f_{\text{PBH}}}{2\pi^2 \Omega_{\text{CDM}} \rho_{\text{cr}}} \frac{1}{A_s}}$$

For the cosmological parameters to be varied, we sample different values of σ_8 , i.e., the normalization of the linear power spectrum, and n_{eff} , the slope of the power spectrum evaluated at the scale probed by the Lyman- α forest ($k_\alpha = 0.009$ s/km) [70–72]. We included five different simulations for both σ_8 ([0.754, 0.904]) and n_{eff} ([−2.3474, −2.2674]). Additionally, we included simulations corresponding to different values for the instantaneous reionization redshift, i.e., $z_{\text{reio}} = \{7, 9, 15\}$.

Regarding the astrophysical parameters, we modeled the IGM thermal history with amplitude T_0 and slope γ of its temperature-density relation, parameterized as $T = T_0(1 + \delta_{\text{IGM}})^{\gamma-1}$, with δ_{IGM} being the IGM overdensity [73]. We use simulations with temperatures at mean density $T_0(z = 4.2) = \{6000, 9200, 12600\}$ K, evolving with redshift, and a set of three values for the slope of the temperature-density relation, $\gamma(z = 4.2) = \{0.88, 1.24, 1.47\}$. The redshift evolution of both T_0 and γ are parameterized as power laws, such that $T_0(z) = T_0^A[(1+z)/(1+z_p)]^{T_0^S}$ and $\gamma(z) = \gamma^A[(1+z)/(1+z_p)]^{\gamma^S}$, where the pivot redshift z_p is the redshift at which most of the Lyman- α forest pixels are coming from ($z_p = 4.5$). The reference thermal history is defined by $T_0(z = 4.2) = 9200$ and $\gamma(z = 4.2) = 1.47$ [74].

Furthermore, we considered the effect of ultraviolet (UV) fluctuations of the ionizing background, controlled by the parameter f_{UV} . Its template is built from three simulations with $f_{\text{UV}} = \{0, 0.5, 1\}$, where $f_{\text{UV}} = 0$ corresponds to a spatially uniform UV background [68]. We also included 9 grid points obtained by rescaling the mean Lyman- α flux $\bar{F}(z)$, namely $\{0.6, 0.7, 0.8, 0.9, 1.0, 1.1, 1.2, 1.3, 1.4\} \times \bar{F}_{\text{REF}}$, with reference values given by SDSS-III/BOSS measurements [75]. We also considered 8 additional values, obtained by rescaling the optical depth $\tau = -\ln \bar{F}$, i.e. $\{0.6, 0.7, 0.8, 0.9, 1.1, 1.2, 1.3, 1.4\} \times \tau_{\text{REF}}$.

Concerning the PBH properties, we extracted the flux power spectra from 12 hydrodynamic simulations (512^3 particles; 20 comoving Mpc/ h box length) corresponding to the following PBH mass and fraction products: $\log(M_{\text{PBH}}f_{\text{PBH}}) = \{1.0, 1.5, 2.0, 2.2, 2.3, 2.4, 2.5, 2.6, 2.7, 3.0, 3.5, 4.0\}$. For this set of simulations, astrophysical and cosmological parameters have been fixed to their reference values, and the equivalent Λ CDM flux power was also determined.

Our datasets are the MIKE and HIRES/KECK samples of quasar spectra, at $z = \{4.2, 4.6, 5.0, 5.4\}$, in 10 k -bins in the range [0.001 – 0.08] s/km, with spectral resolution of 13.6 and 6.7 s/km [53]. We consider only measurements at $k > 0.005$ s/km, to avoid systematic uncertainties due to continuum fitting. Moreover, we did not use MIKE highest redshift bin. [53]. We thus have a total of 49 (k, z) data-points.

Results and Discussion. We obtain our results by maximising a Gaussian likelihood with a Monte Carlo Markov Chain (MCMC) approach, using the publicly available MCMC sampler `emcee` [77]. We adopted Gaussian priors on the mean fluxes $\bar{F}(z)$, centered on their reference values, with standard deviation $\sigma = 0.04$ [68], and on σ_8 and n_{eff} , centered on their Planck values [69], with $\sigma = 0.05$, since the latter two parameters, whereas well constrained by CMB data, are poorly constrained by Lyman- α data alone [63]. We adopt logarithmic priors on $f_{\text{PBH}}M_{\text{PBH}}$ (but our results are not affected by this choice). Concerning the IGM thermal history, we adopt flat priors on both T_0^A and T_0^S , in the ranges $[0, 2] \cdot 10^4$ K and $[-5, 5]$, respectively. When the corresponding $T_0(z)$ are determined, they can assume values not enclosed by our template of simulations. When this occurs, the corresponding values of the flux power spectra are linearly extrapolated. Regarding γ^S and γ^A , we impose flat priors on the corresponding $\gamma(z)$ (in the interval $[1, 1.7]$). The priors on z_{reio} and f_{UV} are flat within the boundaries defined by our grid of simulations.

Parameter	Flat prior on z_{reio}		Gaussian prior on z_{reio}	
	(2σ)	Best Fit	(2σ)	Best Fit
$\bar{F}(z = 4.2)$	[0.35, 0.41]	0.37	[0.35, 0.41]	0.37
$\bar{F}(z = 4.6)$	[0.26, 0.34]	0.28	[0.27, 0.34]	0.28
$\bar{F}(z = 5.0)$	[0.15, 0.25]	0.20	[0.15, 0.23]	0.16
$\bar{F}(z = 5.4)$	[0.03, 0.12]	0.08	[0.04, 0.11]	0.05
$T_0^A [10^4 \text{ K}]$	[0.44, 1.36]	0.72	[0.46, 1.44]	0.84
T_0^S	[-5.00, 3.34]	-4.47	[-5.00, 3.35]	-4.53
γ^A	[1.21, 1.60]	1.51	[1.19, 1.61]	1.44
γ^S	[-2.43, 1.30]	-1.76	[-2.25, 1.51]	4.64
σ_8	[0.72, 0.91]	0.79	[0.72, 0.91]	0.81
z_{reio}	[7.00, 15.00]	14.19	[7.12, 10.25]	9.07
n_{eff}	[-2.40, -2.22]	-2.30	[-2.41, -2.22]	-2.33
f_{UV}	[0.00, 1.00]	0.02	[0.00, 1.00]	0.03
$\log(f_{\text{PBH}} M_{\text{PBH}})$	< 2.24	1.96	< 1.78	0.34
$\chi^2/\text{d.o.f.}$	32/42		33/43	

TABLE I. 2σ limits and best fit values for all the parameters of our analyses, for the two different prior choices on z_{reio} that we adopted. The values for M_{PBH} are expressed in units of M_{\odot} .